

Charge ordering and disordering transitions in $\text{Pr}_{1-x}\text{Ca}_x\text{MnO}_3$ ($x=0.4$) as investigated by optical spectroscopy

Y. Okimoto

Department of Applied Physics, University of Tokyo, Tokyo 113, Japan

Y. Tomioka

Joint Research Center for Atom Technology (JRCAT), Tsukuba, 305, Japan

Y. Onose and Y. Otsuka

Department of Applied Physics, University of Tokyo, Tokyo 113, Japan

Y. Tokura

*Department of Applied Physics, University of Tokyo, Tokyo 113, Japan
and Joint Research Center for Atom Technology (JRCAT), Tsukuba, 305, Japan*

(Received 24 December 1997)

The magnetic-field dependence of optical spectra and their anisotropy have been investigated for a single crystal of $\text{Pr}_{1-x}\text{Ca}_x\text{MnO}_3$ ($x=0.4$) at 30 K. The charge-ordered (CO) state is transformed into a ferromagnetic metallic state by a magnetic field of 6.5 T, which is manifested in a huge change of optical spectra over a wide photon-energy region (0.05 eV–3 eV). The observed change in magnitude and anisotropy of the optical spectra with the external magnetic field has been elucidated in terms of the spin- and orbital-ordering structures in the CO state. [S0163-1829(98)51316-1]

In the course of recent intensive studies, spin-charge-orbital coupled phenomena have been revealed for perovskite-type manganese oxides. The $\text{La}_{1-x}\text{Sr}_x\text{MnO}_3$ system, which has a relatively wide one-electron bandwidth (W), shows a ferromagnetic metallic state¹ mediated by the double-exchange mechanism²⁻⁴ and a large magnetoresistance effect was observed near the Curie temperature (T_C).⁵ In a more distorted perovskite with a smaller W , $\text{Pr}_{1-x}\text{Ca}_x\text{MnO}_3$ ($0.3 \leq x \leq 0.5$) system, however, the metallic (and ferromagnetic) state is no longer present and real space ordering of charge carriers (charge ordering) takes place.^{6,7} Such a charge-ordered (CO) state is accompanied with spin and orbital ordering, the pattern of which is called *CE* type.^{8,9} The robustness of the CO state is very sensitive to the commensurability of the hole concentration with a periodicity of the lattice⁷ and hence most enhanced at the nominal hole concentration $x=1/2$. The deviation of hole concentration from $x=1/2$ weakens the CO state, so that application of an external magnetic field can melt the CO state into a ferromagnetic metallic state, decreasing the resistivity by more than several orders of magnitude.^{6,7}

Measurements of optical spectra are useful in probing the electronic structure of the perovskite-type manganese oxide.¹⁰ In this paper, we adopt a crystal of $\text{Pr}_{1-x}\text{Ca}_x\text{MnO}_3$ ($x=0.4$) as a prototypical charge-ordering system. In addition to the magnetic-field-induced transition,⁶ metal-insulator phase control has recently been demonstrated for the $\text{Pr}_{1-x}\text{Ca}_x\text{MnO}_3$ system, such as the insulator-metal transitions induced by x-ray irradiation,¹¹ photoexcitation,¹² and current injection,¹³ which are all relevant to the charge-disordering transition. We investigate here the variation of the anisotropic electronic structure of the CO state with magnetic field in terms of optical conductivity spectra.

To overview the transport and magnetic properties of the *CE*-type CO state of $\text{Pr}_{1-x}\text{Ca}_x\text{MnO}_3$ ($x=0.4$), we reproduce in Fig. 1(a) the phase diagram in the temperature and magnetic-field plane.⁷ This compound undergoes the charge/orbital-ordering transition at $T_{\text{CO}} \approx 235$ K under zero field, and the nominal Mn^{3+} and Mn^{4+} species are regularly arranged below T_{CO} as shown in Fig. 1(b). Upon the charge ordering, $d_{3x^2-r^2}$ and $d_{3y^2-r^2}$ orbitals at the Mn^{3+} site are alternately ordered in the *ab* plane,⁸ as also shown in Fig. 1(b). As the temperature is decreased, antiferromagnetic spin ordering subsequently occurs [$T_N \approx 170$ K, a closed triangle in Fig. 1 (a)]. The pattern of spin ordering below T_N is so called *CE*-type.^{8,9} (To be precise on the basis of the neutron diffraction measurement,⁸ the direction of the spin is canted from the *c* axis by 20° – 30° .) The fact that T_N is lower than T_{CO} is characteristic of the $\text{Pr}_{1-x}\text{Ca}_x\text{MnO}_3$ system and contrary to the case of the $\text{Nd}_{1/2}\text{Sr}_{1/2}\text{MnO}_3$ system where the similar *CE* type but *concomitant* spin and charge ordering takes place.¹⁴ With the decrease of temperature below T_N , the canted antiferromagnetic ordering occurs at $T_{\text{CA}} \approx 40$ K [an open triangle in Fig. 1(b)]. This order is perhaps a consequence of an incommensurate hole-doping level ($x < 1/2$) and in the $x=1/2$ crystal such a canted magnetic order has not been observed.⁹ Under the external magnetic field, the CO state is transformed into a ferromagnetic metallic state as mentioned before. The hatched region in Fig. 1(a) shows a field-hysteresis characteristic of the first-order phase transition. Hereafter, we show a variation of the optical spectra at 30 K along a route in the *H*-*T* plane shown with an arrow in Fig. 1(a), which causes the charge-ordering/disordering transition.

A crystal of $\text{Pr}_{1-x}\text{Ca}_x\text{MnO}_3$ ($x=0.4$) was grown by the floating-zone method, the details of which have already been

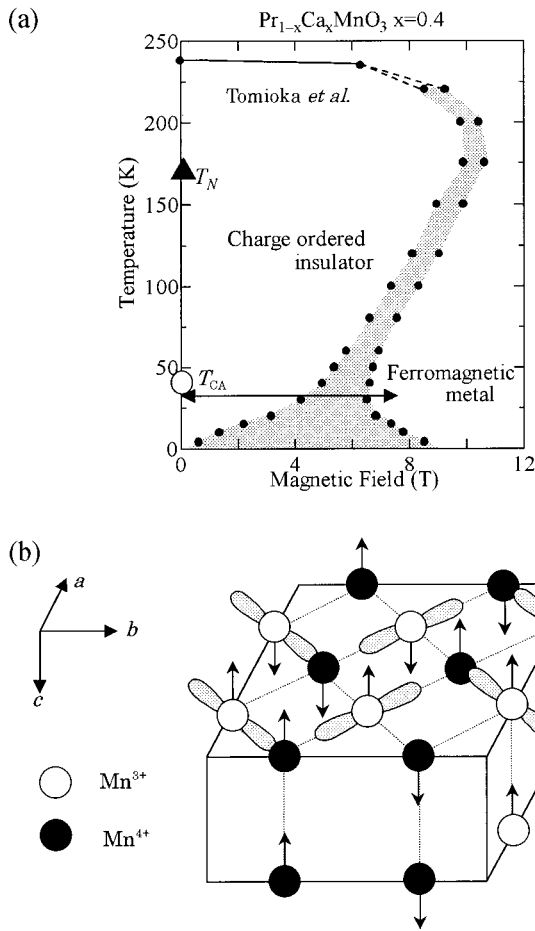


FIG. 1. (a) The temperature and magnetic phase diagram of $\text{Pr}_{1-x}\text{Ca}_x\text{MnO}_3$ ($x=0.4$) derived from Ref. 7. The hatched area shows a field-hysteresis region. A closed triangle denotes the Neel temperature T_N , and an open one the canted antiferromagnetic transition temperature T_{CA} . (b) collinear CE -type spin- and charge-ordering structure. The lobes show the $d_{3x^2-r^2}$ and $d_{3y^2-r^2}$ orbitals (see text).

reported elsewhere.⁷ Inductively coupled plasma atomic emission spectroscopy and chemical titration have confirmed that the obtained crystal has precisely prescribed stoichiometry. Near-normal incidence reflectivity [$R(\omega)$] was measured on the (1 0 0) face of the $x=0.4$ crystal ($Pbnm$ orthorhombic structure) with a typical size of $4\text{mm} \times 5\text{mm} \times 0.5\text{mm}$ using a Fourier transform type spectrometer for the range of 0.05–0.8 eV and grating monochromators for the higher-energy region (0.6–36 eV). For the measurement above 5 eV, we utilized synchrotron radiation at the INS-SOR, Institute for Solid State Physics, University of Tokyo. We measured $R(\omega)$ between 0.01 eV and 3 eV with varying temperature under 0 T. High magnetic-field measurements of $R(\omega)$ between 0.05 eV and 3 eV at 30 K were made with a 7 T split-type superconducting magnet equipped with ZnSe and KRS-5 windows for infrared spectroscopy and quartz ones for visible measurements. The magnetic field was applied along the b axis of the $Pbnm$ orthorhombic lattice [see Fig. 1(b)]. The optical conductivity spectra at various temperatures and magnetic fields were obtained by a Kramers-Kronig (KK) analysis of the respective $R(\omega)$ data.¹⁵ For the analysis,¹⁶ we assumed the constant reflectivity below the

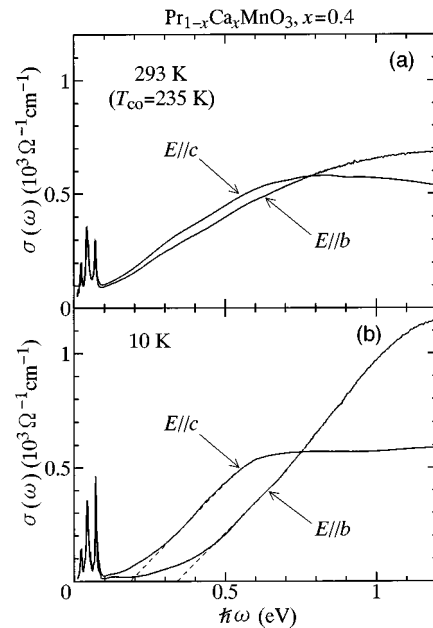


FIG. 2. The anisotropy ($E\parallel b$ and $E\parallel c$ polarization) of the optical conductivity in a single crystal of $\text{Pr}_{1-x}\text{Ca}_x\text{MnO}_3$ ($x=0.4$) at (a) 293 K and (b) 10 K.

lowest photon energy investigated and ω^{-4} extrapolation above 36 eV. The measurements of magnetic susceptibility were done with a superconducting quantum interference device magnetometer. Resistivity was measured by the conventional four-probe technique.

We show in Fig. 2 optical the conductivity spectrum [$\sigma(\omega)$] in $\text{Pr}_{1-x}\text{Ca}_x\text{MnO}_3$ ($x=0.4$) for $E\parallel b$ and $E\parallel c$ at 293 K (a) and 10 K (b). (Spiky structures below 0.06 eV are due to optical-phonon modes.) At 293 K above T_{CO} , anisotropy of $\sigma(\omega)$ is quite small and the minute polarization dependence is perhaps due to the orthorhombic distortion. With the decrease of temperature from 293 K to 10 K, the spectral weight of both the b and c axis polarized $\sigma(\omega)$ below ≈ 0.2 eV is suppressed at 10 K indicating an opening of the charge gap in the CO state. Such a temperature dependence of $\sigma(\omega)$ resembles that of the two-dimensional CO system, $\text{La}_{5/3}\text{Sr}_{1/3}\text{NiO}_4$.¹⁸ In the CO state at 10 K (viewed as the ground state), the difference between the b and c axes polarized $\sigma(\omega)$ becomes large reflecting the anisotropy of the ordering pattern of the charge, spin, and orbitals [see Fig. 1(b)]. The most notable anisotropic feature is that each $\sigma(\omega)$ has a different onset energy (Δ). To be more quantitative, we have estimated each Δ (Δ_b and Δ_c) by extrapolating linearly the rising part of the b and c axes polarized $\sigma(\omega)$ to the abscissa as shown by dashed lines in Fig. 2(b). It is reasonable to consider that the Δ_b means that the charge transfer energy arising from the transition of $d_{3x^2-r^2}$ (or $d_{3y^2-r^2}$) electron to the neighboring Mn^{4+} site with a parallel spin [see Fig. 1(b)]. The $d_{3x^2-r^2}$ ($d_{3y^2-r^2}$) electron can hardly hop along the c axes due to a small transfer integral as well as to a large on-site Coulomb energy. The excess electrons which are introduced into the CE -type CO state by decreasing from $x=1/2$ are likely to occupy the $d_{3z^2-r^2}$ orbital of the Mn^{4+} site,⁸ so that the Δ_c originates from the intersite transition of such excess $d_{3z^2-r^2}$ electrons. The fact of $\Delta_c < \Delta_b$ implies that the effective intersite Coulomb cor-

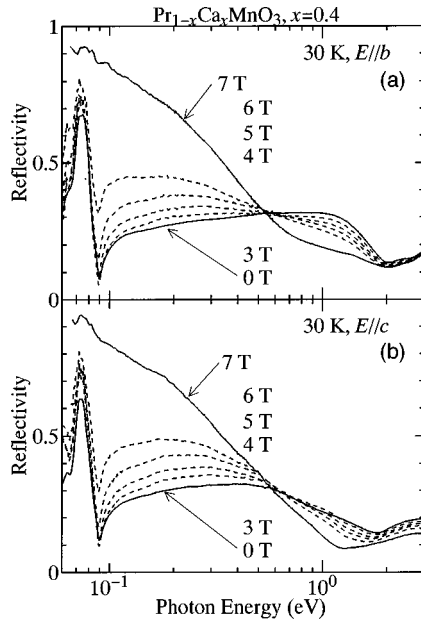


FIG. 3. The magnetic-field dependence of (a) b -polarized and (b) c -polarized reflectivity spectra of $\text{Pr}_{1-x}\text{Ca}_x\text{MnO}_3$ ($x=0.4$) at 30 K.

relation is larger for the in plane than that for the c axes in such a discommensurate CO state. Under these circumstances, the gap energy of the density of states should be assigned to Δ_c (≈ 0.18 eV) in the ground state rather than Δ_b . This gap energy is comparable to that of CO state of other $3d$ transition metal oxides, e.g., Fe_3O_4 (≈ 0.14 eV) (Ref. 19) and $\text{La}_{5/3}\text{Sr}_{1/3}\text{NiO}_4$ (≈ 0.24 eV).¹⁸

The next issue to be discussed is the variation and collapse of the gap structure in the course of the magnetic field-induced insulator-metal transition (IMT) in a $\text{Pr}_{1-x}\text{Ca}_x\text{MnO}_3$ ($x=0.4$) crystal at 30 K. (Both the b - and c -polarized optical spectra scarcely changes from 10 K to 30 K.) As displayed in Fig. 1(a), the IMT at 30 K is observed at 6.4 T and 4.2 T in the field-increasing and decreasing run, respectively. We show the magnetic-field dependence of b - and c -polarized $R(\omega)$ at 30 K in Figs. 3(a) and (b), respectively. A spiky structure around 0.06 eV is due to the highest-lying oxygen phonon mode. In both the b - and c -polarized $R(\omega)$, the infrared reflectivity is gradually increased with a field up to 6 T, and abruptly transformed into the metallic one between 6 and 6.5 T. Such a huge spectral change with an external magnetic field over a wide energy region up to 3 eV (as it were *magnetochromism*) has seldom been observed so far. We show the b - and c -polarized $\sigma(\omega)$ spectra deduced by KK analysis in Figs. 4(a) and (b), respectively. With increasing magnetic field, the onset of $\sigma(\omega)$ gradually shifts to lower energy, and at 7 T the $\sigma(\omega)$ undergoes a large change into a metallic band, as expected from the variation of $R(\omega)$. We estimated Δ by means of the same extrapolating procedure as in the analysis of 10 K spectra [Fig. 2(b)]. In Fig. 5(a) is shown a variation of the Δ value with a magnetic field at 30 K both for the field-increasing and decreasing runs.

For comparison, we show in Fig. 5(b) the magnetic-field dependence of resistivity (ρ) along the b axis at 30 K. The applied magnetic field was parallel to the b axis as in the optical measurements. The ρ steeply drops between 5 and 7

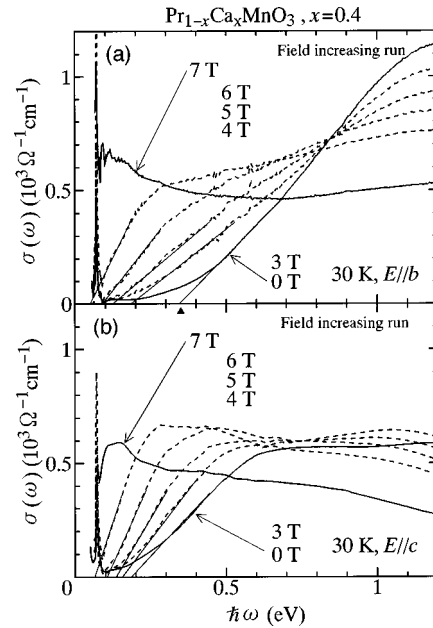


FIG. 4. The magnetic-field dependence of (a) b -polarized and (b) c -polarized optical conductivity spectra at 30 K deduced by Kramers-Kronig analysis.

T in the field-increasing run. Above 6.5 T the ρ -value is metallic ($\approx 5 \times 10^{-4}$ Ω cm) and no longer affected by further increasing the field, indicating the occurrence of the fully spin-polarized metallic state. The observed variation of optical spectra is consistent with this magnetoresistive behavior. As mentioned above, the Δ value (30 K, 0 T) is different between the b and c axes by ≈ 0.18 eV. The difference is gradually decreased with a magnetic field and both the Δ_b and Δ_c values become zero almost continuously at 6.5 T in the field-increasing run. These results clearly indicate that the order parameter of the CO state, which can

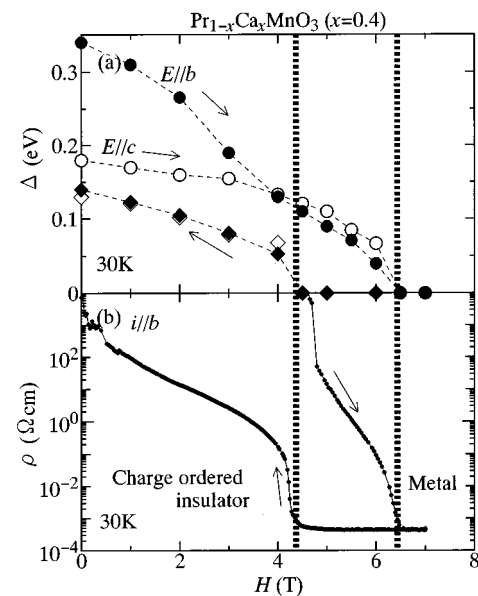


FIG. 5. (a) The magnetic-field dependence of the Δ_b (closed symbols) and Δ_c (open ones) in the field-increasing run (circles) and decreasing run (squares) for $\text{Pr}_{1-x}\text{Ca}_x\text{MnO}_3$ ($x=0.4$). (b) The magnetic-field dependence of resistivity (ρ).

hardly be probed by resistivity measurements, continuously decreases and the difference between Δ_b and Δ_c is suppressed with the magnetic field. In the field-decreasing run, the gap opening is observed below the critical field between 4.5 and 4 T, in accord again with the field-hysteretic behavior of the resistivity. However, the Δ_b and Δ_c are comparable and obviously less than the Δ_b in the field-increasing run, as shown in an inset of Fig. 5(a). This irreversible behavior is perhaps due to the strong first-order nature of the present field-induced transition, but consistent with a difference in the resistivity values of the CO state between the field-increasing and decreasing runs.

It is worth noting here that Δ_b and Δ_c gradually change with a magnetic field while $\sigma(\omega)$ [or $R(\omega)$] drastically changes from a gaplike to a metallic feature around 6.5 T. Such a large energy-scale change upon the IMT is reminiscent of the Mott transition in the electron correlated system. As in a barely metallic state near the Mott transition, the spectral shape of $\sigma(\omega)$ at 7 T, where the metallic ferromagnetic state is realized, is only moderately dependent on ω , being far from a simple Drude shape. The value of the dc conductivity [$\sigma(0)$] at 30 K and 7 T is $\approx 2 \times 10^3 \Omega^{-1} \text{ cm}^{-1}$ [see Fig. 5(b)] and merely about twice the value of $\sigma(\omega)$ at 0.05 eV. These results imply that the charge dynamics in the field-induced metallic state is highly diffuse or incoherent,²⁰ which is also consistent with the results of $\text{La}_{1-x}\text{Sr}_x\text{MnO}_3$

near the metal-insulator phase boundary.¹⁰

In summary, we have observed the variation of optical spectra and their anisotropy with magnetic field for a single crystal of $\text{Pr}_{1-x}\text{Ca}_x\text{MnO}_3$ ($x=0.4$). In the ground state of the CO state (10 K), Δ_c (the onset energy of c -polarized optical conductivity) is smaller than Δ_b , which is anticipated from the proposed spatial pattern of the charge and orbital ordering in the CO state. The optical gap energy at 10 K is estimated as ≈ 0.18 eV, which is comparable to other CO systems. We have investigated the electronic-structural change in the course of the magnetic-field-induced insulator-metal transition at 30 K. Both the b - and c -polarized spectra drastically change at 7 T over a wide photon-energy region (0.05 eV–3 eV). The magnitude of Δ_b and Δ_c obtained from the respective $\sigma(\omega)$ gradually decrease with a magnetic field and disappears at 6.5 T. These results indicate the rather continuous change in the electronic structure from the anisotropic CO state to the isotropic ferromagnetic metal with increasing the magnetic field.

We would like to thank S. Ishihara, T. Arima, and T. Katsufuji for enlightening discussions. This work was supported in part by Grant-in-Aids for Scientific Research from the Ministry of Education, Science, Sport, and Culture, Japan, and by the New Energy and Industrial Technology Development Organization of Japan (NEDO).

-
- ¹G. H. Jonker and J. H. van Santen, *Physica (Amsterdam)* **16**, 337 (1950).
- ²C. Zener, *Phys. Rev.* **82**, 403 (1951).
- ³P. W. Anderson and H. Hasegawa, *Phys. Rev.* **100**, 675 (1955).
- ⁴P. -G. de Gennes, *Phys. Rev.* **118**, 141 (1960).
- ⁵Y. Tokura, A. Urushibara, Y. Mirotomo, T. Arima, A. Asamitsu, G. Kido, and N. Furukawa, *J. Phys. Soc. Jpn.* **63**, 3931 (1994), and references cited therein.
- ⁶Y. Tomioka, A. Asamitsu, Y. Moritomo, and Y. Tokura, *J. Phys. Soc. Jpn.* **64**, 3626 (1995).
- ⁷Y. Tomioka, A. Asamitsu, H. Kuwahara, and Y. Tokura, *Phys. Rev. B* **53**, R1689 (1996).
- ⁸Z. Jirak, S. Krupicka, Z. Simsa, M. Dlouha, and Z. Vlatislav, *J. Magn. Magn. Mater.* **53**, 153 (1985).
- ⁹H. Yoshizawa, H. Kawano, Y. Tomioka, and Y. Tokura, *J. Phys. Soc. Jpn.* **52**, 3626 (1995).
- ¹⁰Y. Okimoto, T. Katsufuji, T. Ishikawa, A. Urushibara, T. Arima, and Y. Tokura, *Phys. Rev. Lett.* **75**, 109 (1995); S. G. Kim, J. Y. Gu, H. S. Choi, G. W. Park, and T. W. Noh, *ibid.* **77**, 1877 (1996); S. G. Kaplan, M. Quijada, H. D. Drew, D. B. Tanner, G. C. Xiong, R. Ramesh, C. Won, and T. Venkatesan, *ibid.* **77**, 2081 (1996).
- ¹¹V. Kiryukhin, D. Casa, J. P. Hill, B. Keimer, A. Bigilante, Y. Tomioka, and Y. Tokura, *Nature (London)* **386**, 813 (1997).
- ¹²K. Miyano, T. Tanaka, Y. Tomioka, and Y. Tokura, *Phys. Rev. Lett.* **78**, 4257 (1997).
- ¹³A. Asamitsu, Y. Tomioka, and Y. Tokura, *Nature (London)* **388**, 50 (1997).
- ¹⁴H. Kuwahara, Y. Tomioka, A. Asamitsu, Y. Moritomo, and Y. Tokura, *Science* **270**, 961 (1995).
- ¹⁵As for the $R(\omega)$ data, we connected the room-temperature data above 3 eV with each temperature data.
- ¹⁶We measured $R(\omega)$ under Voigt-geometry ($\mathbf{k} \perp \mathbf{H}$) for 0.05 eV–0.8 eV and Faraday geometry ($\mathbf{k} \parallel \mathbf{H}$) 0.6 eV–3 eV. As for the manganese oxide, the magnitude of $\epsilon_{xy}(\omega)$ in the low-energy (<4 eV) region is much smaller than that of diagonal part (Ref. 17) due partly to no orbital moment for the e_g electron and hence to minimal spin-orbit coupling, so that we may neglect an off-diagonal component of dielectric tensor [$\epsilon_{xy}(\omega)$] in executing KK analysis.
- ¹⁷S. Yamaguchi, Y. Okimoto, and Y. Tokura (unpublished).
- ¹⁸T. Katsufuji, T. Tanabe, T. Ishikawa, Y. Fukuda, T. Arima, and Y. Tokura, *Phys. Rev. B* **54**, R14 230 (1996).
- ¹⁹S.-K. Park, T. Ishikawa, and Y. Tokura (unpublished).
- ²⁰S. Ishihara and N. Nagaosa, *J. Phys. Soc. Jpn.* **66**, 3678 (1997).